Electronic Supplementary Information (ESI)

Hybrid Cobalt(II) Fluoride Derived from Bimetallic Zeolitic Imidazolate Framework as a High-Performance Cathode for Lithium–Ion Batteries

Qiuxia Cheng,[†] Yueying Chen,[†] Xiaoming Lin,[*,†,§] Jincheng Liu,[‡] Zhongzhi Yuan[*,†] and Yuepeng Cai[*,†]

[†] *Guangzhou Key Laboratory of Materials for Energy Conversion and Storage, School of Chemistry, South China Normal University, Guangzhou 510006, P. R. China*

[‡] *EVE Energy Co. Ltd, Huizhou, Guangdong 516006, P.R. China*

[§] *School of Environment and Energy, South China University of Technology, Guangzhou, Guangdong 510006, P.R. China*

*Author to whom correspondence should be addressed. E-mail: linxm@scnu.edu.cn (X. Lin); yuanzz@scnu.edu.cn (Z. Yuan); caiyp@scnu.edu.cn (Y. Cai).

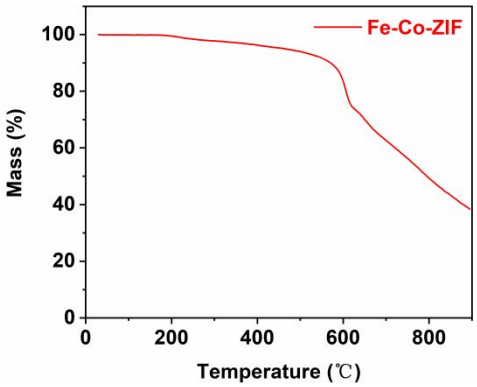

Figure S1. TG curve under N_2 of Fe-Co-ZIF.

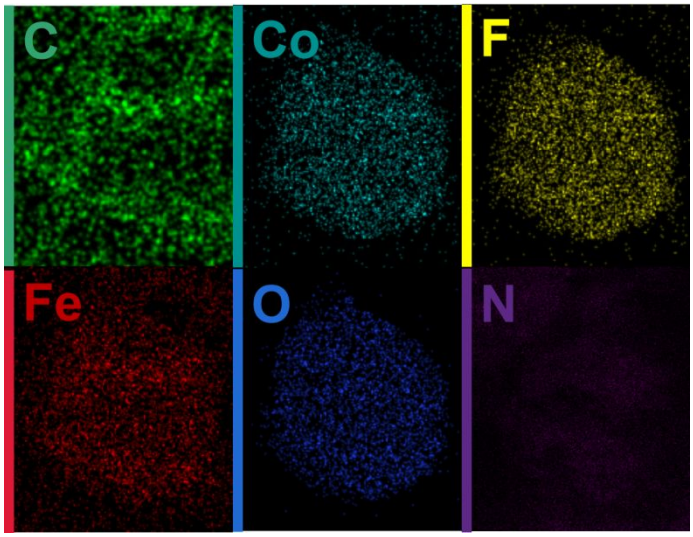

Figure S2 EDS mapping results.

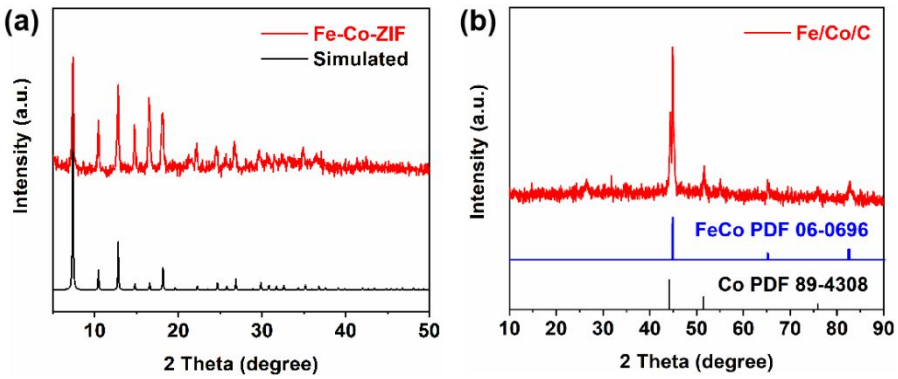

Figure S3 XRD patterns of (a) Fe-Co-ZIF, (b) Fe/Co/C.

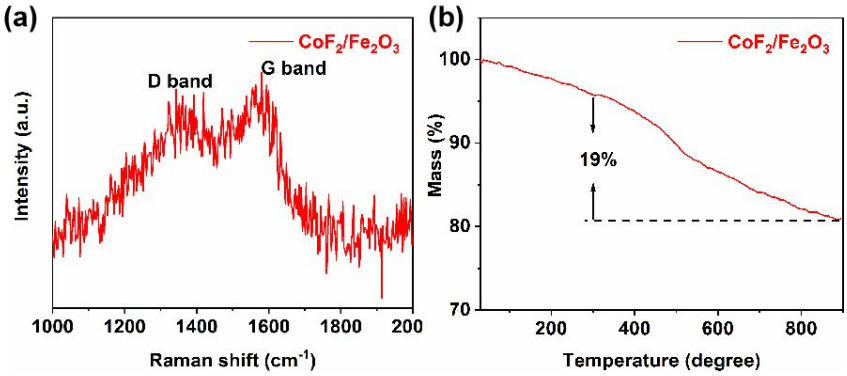

Figure S4. Characterization of CoF_2/Fe_2O_3. (a) Raman spectrum. (b) TG curve in air.

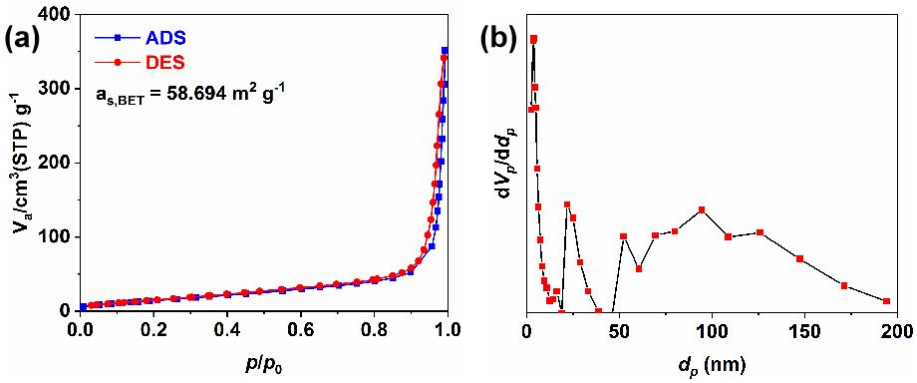

Figure S5. (a) N_2 adsorption−desorption isotherm. (b) Pore size.

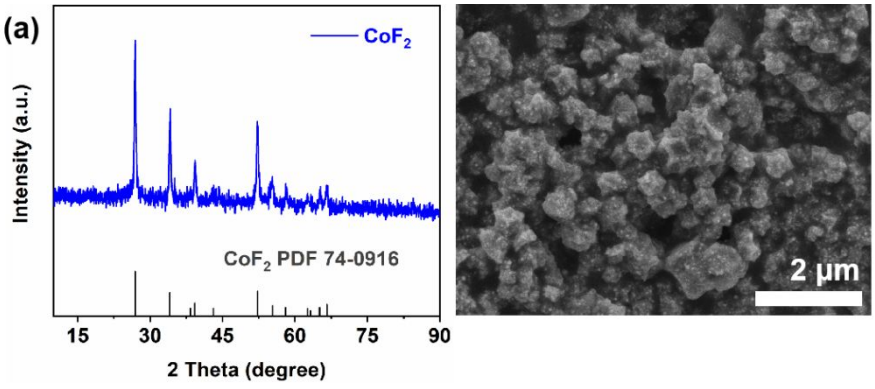

Figure S6. Characterization ZIF-derived CoF_2. (a) XRD, (b) SEM image.

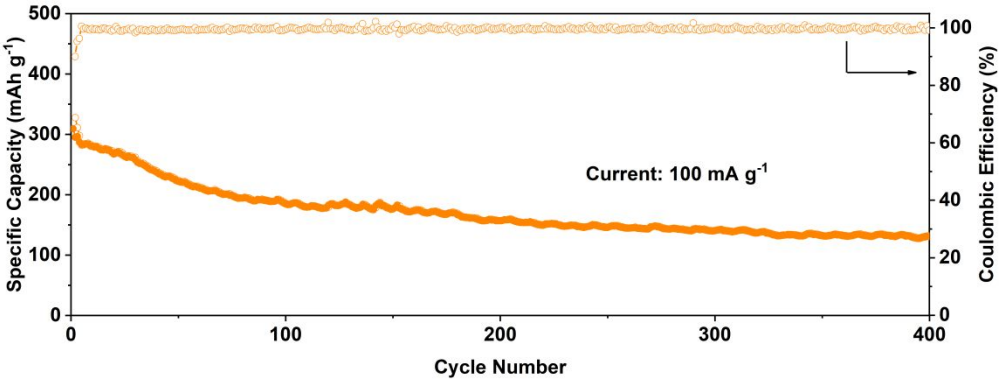

Figure S7. Cycling specific capacity and coulomb efficiency of CoF_2/Fe_2O_3 sample.

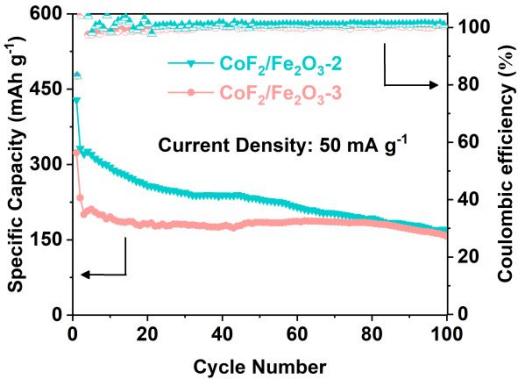

Figure S8. Electrochemical performance of CoF_2/Fe_2O_3-2 and CoF_2/Fe_2O_3-3.

Table S1 Comparison of specific capacity of cobalt fluoride materials.

Name	Voltage range (V)	Current (mA g^{-1})	Cycle number	Capacity (mAh g^{-1})	Reference
CoF_2	1.0 − 4.5	55.3	30	50	(S1)
CoF_2(NC3100)	1.0 − 4.3	50	10	175	(S2)
CoF_2/CNT	1.0 − 4.0	100	200	334.8	(S3)
CoF_2	1.2 − 4.8	20	25	50	(S4)
$Fe_{(1-x)}Co_xF_3$/MWCNT (x=0.04)	2.0 − 4.5	47.4	50	187.9	(S5)
CoF_2 (S_{200})	1.0 − 4.8	20	30	127.4	(S6)
CoF_2/Fe_2O_3	1.2 − 4.5	50	100	198.1	This work

Table S2 R_{ct} values of the as-prepared materials before and after cycles.

Name	Fresh	After 50 cycles
	R_{ct}	R_{ct}
CoF_2	293 Ω	80 Ω
CoF_2/Fe_2O_3	196 Ω	78 Ω

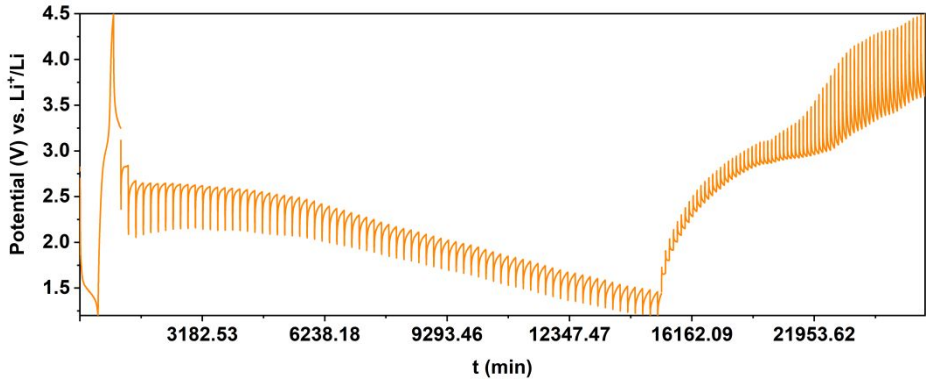

Figure S9. GITT result during the whole charge-discharge process.

Table S3 D_{Li^+} camparsion of various fluoride electrods.

Method	Name	Magnitude of D_{Li^+} (m^2 s^{-1})	Reference
EIS	$Fe_{(1-x)}Co_xF_3$/MWCNT	$10^{-12} \sim 10^{-11}$	(S5)
	$Fe_{1-x}Mn_xF_3$•0.33H_2O/C	10^{-16}	(S7)
GITT	M-CF_x-5	$10^{-12} \sim 10^{-11}$	(S8)
	FFH-P	$10^{-13} \sim 10^{-12}$	(S9)
	CoF_2/Fe_2O_3	$10^{-13} \sim 10^{-12}$	This work

Reference

(S1) Tan, J.; Liu, L.; Guo, S.; Hu, H.; Yan, Z.; Zhou, Q.; Huang, Z.; Shu, H.; Yang, X.; Wang, X. The Electrochemical Performance and Mechanism of Cobalt (II) Fluoride as Anode Material for Lithium and Sodium Ion Batteries. *Electrochim. Acta* **2015**, *168*, 225-233.

(S2) Teng, Y. T.; Pramana, S. S.; Ding, J.; Wu, T.; Yazami, R. Investigation of the Conversion Mechanism of Nanosized CoF_2. *Electrochim. Acta* **2013**, *107*, 301-312.

(S3) Wang, X. R.; Gu W. T.; Lee, J. T.; Nitta, N.; Benson, J.; Magasinski, A.; Schauer, M. W.; Yushin, G. Carbon Nanotube–CoF_2 Multifunctional Cathode for Lithium Ion Batteries: Effect of Electrolyte on Cycle Stability, *Small* **2015**, *11*, 5164–5173.

(S4) Armstrong, M. J.; Panneerselvam, A.; O'Regan, C.; Morris, M. A.; Holmes, J. D. Supercritical-Fluid Synthesis of FeF_2 and CoF_2 Li-Ion Conversion Materials. *J. Mater. Chem. A* **2013**, *1*, 10667-10676.

(S5) Li, J.; Xu, S.; Huang, S.; Lu, L.; Lan, L.; Li, S. In Situ Synthesis of $Fe_{(1-x)}Co_xF_3$/MWCNT Nanocomposites with Excellent Electrochemical Performance for Lithium-Ion Batteries. *J Mater Sci.* **2018**, *53*, 2697-2708.

(S6) Guan, Q.; Cheng, J.; Li, X.; Ni, W.; Wang, B. Porous CoF_2 Spheres Synthesized by a One-Pot Solvothermal Method as High Capacity Cathode Materials for Lithium-Ion Batteries. *Chin. J. Chem.* **2017**, *35*, 48-54.

(S7) Ding, J.; Zhou, X.; Wang, H.; Yang, J.; Gao, Y.; Tang, J. Mn-Doped $Fe_{1-x}Mn_xF_3.0.33H_2O$/C Cathodes for Li-Ion Batteries: First-Principles Calculations and Experimental Study. *ACS Appl. Mater. Interfaces* **2019**, *11*, 3852-3860.

(S8) Zhou, P.; Weng, J.; Liu, X.; Li, Y.; Wang, L.; Wu, X.; Zhou, T.; Zhou, J.; Zhuo, S. Urea-Assistant Ball-Milled CF as Electrode Material for Primary Lithium Battery with Improved Energy Density and Power Density. *J. Power Sources* **2019**, *414*, 210-217.

(S9) Chen, G.; Zhou, X.; Bai, Y.; Yuan, Y.; Li, Y.; Chen, M.; Ma, L.; Tan, G.; Hu, J.; Wang, Z.; Wu, F.; Wu, C.; Lu, J. Enhanced Lithium Storage Capability of $FeF_3 \cdot 0.33H_2O$ Single Crystal with Active Insertion Site Exposed. *Nano Energy* **2019**, *56*, 884-892.